# Influence of dense granular columns and liquefiable soil stratigraphic variations on the performance of overlying structures

Caroline Bessette, S.M.ASCE<sup>1</sup>; Lianne Brito, S.M.ASCE<sup>2</sup>; Shideh Dashti, M.ASCE<sup>3</sup>; Abbie Liel, F.ASCE<sup>4</sup>

<sup>1</sup>Graduate Research Assistant, Department of Civil, Environmental, and Architectural Engineering, Univ. of Colorado Boulder, Boulder, CO. E-mail: <a href="mailto:caroline.bessette@colorado.edu">caroline.bessette@colorado.edu</a>
<sup>2</sup>Graduate Research Assistant, Department of Civil, Environmental, and Architectural Engineering, Univ. of Colorado Boulder, Boulder, CO. E-mail: <a href="mailto:lianne.brito@colorado.edu">lianne.brito@colorado.edu</a>
<sup>3</sup>Associate Professor, Department of Civil, Environmental, and Architectural Engineering, Univ. of Colorado Boulder, Boulder, CO 80309. E-mail: <a href="mailto:shideh.dashti@colorado.edu">shideh.dashti@colorado.edu</a>
<sup>4</sup>Professor, Department of Civil, Environmental, and Architectural Engineering, Univ. of Colorado Boulder, Boulder, CO 80309. E-mail: <a href="mailto:abbie.liel@colorado.edu">abbie.liel@colorado.edu</a>

### **ABSTRACT**

The current state of practice for designing dense granular columns (DGCs) relies heavily on simplified procedures that assume free-field conditions (no structure or slope) and uniformly layered, level soil deposits composed of clean sand. These guidelines ignore stratigraphic variabilities in the permeability, groundwater table, layer thickness, or relative density of soil layers commonly found in natural deposits. Prior research has shown that such variability can significantly influence the contribution of different mechanisms of displacement, excess pore water pressure generation and redistribution, formation of soil ejecta at the ground surface, accelerations, and subsequent damage to the foundation and structure. These effects and the implications on system performance are poorly understood and hence, not considered in the design of mitigation strategies. In this paper, fully-coupled, three-dimensional (3D), nonlinear dynamic finite-element analyses in OpenSees, validated with centrifuge models, are performed to evaluate fundamentally how DGCs influence the seismic performance of sites with realistic stratigraphy and their overlying shallow-founded structures. The effectiveness of drainage and reinforcement provided by DGCs is shown to depend strongly on the heterogeneity of the soil profile. Draining DGCs are shown to have the potential to effectively reduce the permanent settlement of the foundation compared to an unmitigated structure. In addition, drains with an area replacement ratio  $(A_r)$  greater than 20% significantly reduced the severity of ejecta (quantified through hydraulic gradients) and excess pore pressure ratios in the liquefiable layers. This reduction was especially effective in the case when DGCs were accompanied by densification. However, treatment could adversely impact the acceleration demand transferred to the superstructure due to reduced damping and increased soil stiffness. The results highlight the critical importance of considering stratigraphic variations in the design of mitigation strategies that holistically improve the performance of the soil-foundation-structure system.

### INTRODUCTION

Previous experimental studies and case histories have shown that dense granular columns (DGCs) effectively mitigate the liquefaction hazard through a combination of enhanced drainage, shear reinforcement, and at times densification (Badanagki et al. 2019, Nikolaou et al. 2016).

However, existing simplified procedures for assessing seismic settlements in liquefiable soils and evaluating mitigation effectiveness primarily focus on the behavior of uniformly layered, level deposits of clean sand. These methodologies raise several practical concerns. First, they fail to account for stratigraphic variabilities in terms of permeability, layer thickness, or relative density (Ishihara 1985, Kokusho and Fujita 2011, Badanagki et al. 2019), commonly encountered in natural depositional environments. Second, these procedures often ignore interactions among various layers, the mitigation technique, and an overlying structure.

Prior research has shown that lateral spreads induced by liquefaction can develop on very gentle slopes, leading to displacements of up to 2 m (O'Rourke and Lane 1989), posing significant risks to lifelines and infrastructures. However, it is unclear how variations in soil layer thickness (a buried slope) may induce lateral deformations in a liquefiable site. Additionally, the severity of liquefaction manifestation can be strongly influenced, if not governed, by cross-layer interactions within the soil profile, as observed in the 2010-2011 Christchurch, New Zealand earthquake sequence (Cubrinovski 2017). This case study highlighted that natural deposits are often stratified with thin silt layers that create sharp changes in permeability, affecting the continuity of critical layers, the formation of soil ejecta at the ground surface, or, in general, surface manifestation of liquefaction. Laboratory experiments or numerical studies have further supported these findings, suggesting that spatial variability can significantly influence lateral or vertical ground deformations, surface ejecta, and damage to inelastic structures (Luque and Bray 2017, Badanagki et al. 2018, Beyzaei et al. 2018). These effects are not included in the existing triggering and settlement procedures in the free-field. Furthermore, current mitigation design procedures based on free-field conditions are inadequate near structures, as shallow-founded building structures can notably impact initial static stress conditions, flow paths, and induced dynamic stresses, hence, the consequences of liquefaction. Overall, the contribution of stratigraphic variability to the performance of the soil-foundation system and the effectiveness of mitigation in those conditions remain poorly understood.

In this paper, fully-coupled, 3D, nonlinear dynamic finite-element analyses (FEAs) in OpenSees, validated with centrifuge experiments, are used to investigate the impact of DGCs on key engineering demand parameters that capture the seismic response of shallow-founded structures on realistically stratified soil deposits.

# **CENTRIFUGE TESTING PROGRAM**

A series of centrifuge experiments was conducted at the University of Colorado Boulder's (CU's) 5.5 m-radius, 400 g-ton centrifuge facility to evaluate the seismic response of a multi-degree-of-freedom (MDOF) and potentially inelastic structures on layered, liquefiable deposits. To verify the numerical simulations, a range of centrifuge tests with and without DGCs (Badanagki et al. 2018, 2019, Tiznado et al., 2020) were considered. For brevity, this paper only presents the detailed validation results for a centrifuge test without mitigation, as shown in Figure 1a. The test modeled a 3-story moment-resisting steel frame, simplified 3DOF, shallow-founded structure. This structure was placed on a 1-m thick mat foundation with a footprint size of 9.56 m x 9.56 m with a bearing pressure of 80 kPa (Olarte et al. 2017). The soil profile consisted of a 10 m-thick, dense Ottawa F65 sand layer dry pluviated at a relative density ( $D_r$ ) of approximately 90% at the bottom, a 6 m-thick, potentially liquefiable layer of loose Ottawa sand with a  $D_r \approx 40\%$  in the middle, and a 2-m thick layer of dense Monterey 0/30 sand layer at a  $D_r \approx 90\%$  at the top, which acted as a draining crust. The properties of the soil layers are available in Olarte et al. 2017. The

experiment was carried out using a flexible-shear-beam (FSB) container, and the model was spun to a centrifugal acceleration of 70 g. A servo-hydraulic shake table was utilized to apply a series of 1D horizontal ground motions to the base of the container during flight. Figure 1b shows the acceleration time history of the first major motion that will be used for validation: the 1995 Kobe earthquake recorded at the Takatori station.

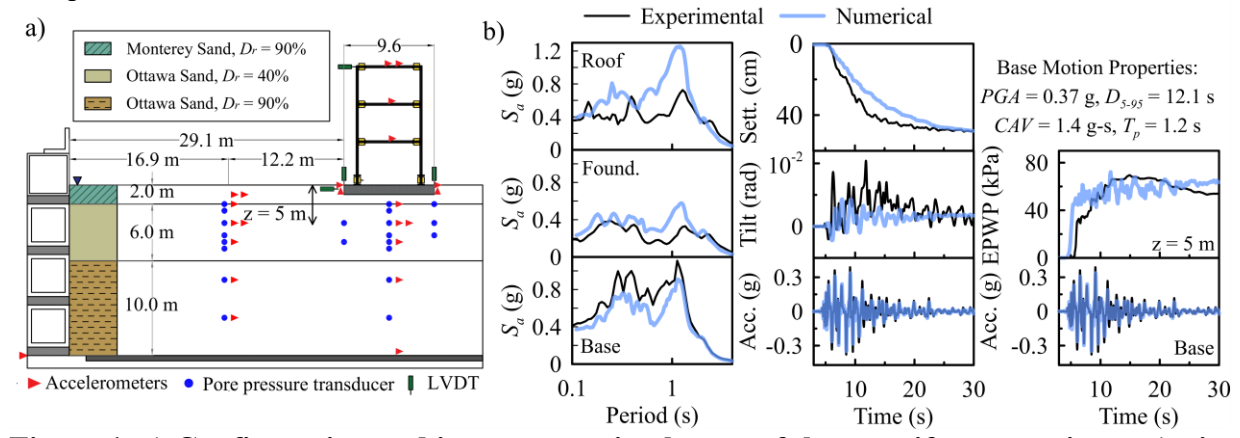


Figure 1. a) Configuration and instrumentation layout of the centrifuge experiment (units are in prototype scale meters), b) Comparison of experimental and numerical results in terms of 5%-damped acceleration response spectra ( $S_a$ ) on the structure, foundation, and base, foundation settlement and tilt time histories, and excess pore water pressure (EPWP) time histories in the middle of the liquefiable layer (z = 5 m) during the Kobe motion.

# NUMERICAL SIMULATIONS

Three-dimensional (3D), fully-coupled, effective stress, nonlinear finite element (FE) simulations were performed in the object-oriented, parallel computation platform OpenSEES (Mazzoni et al. 2006) on the Alpine supercomputer at CU.

The pressure-dependent, multi-yield surface, version 2, soil constitutive model (PDMY02) implemented in OpenSEES by Elgamal et al. (2002) and Yang et al. (2008) was used to simulate the nonlinear response of all granular soil layers. The calibrated model parameters used for the soil layers were adopted from Hwang et al. (2021). The soil elements were modeled with higher-order 20-8 nodes, brick elements with u-p formulation, and the fluid bulk modulus was assumed to be  $2\times10^6$  kPa at atmospheric pressure. To exploit symmetry in the direction perpendicular to shaking (i.e., *y*-axis), only half of the physical model was simulated, as shown in Figure 2a.

The foundation elements consisted of 20-8 node brick u-p elements with linear-elastic material, and the fluid mass density of the foundation was set to zero to prevent excess pore pressure. The MDOF structure was modeled using elastic beam-column elements to match the design bearing pressure. The acceleration time history of the Kobe motion recorded at the base of the container was applied to the base nodes. Additional information and discussion on the soil, structure, damping properties, and model boundary conditions are available in Figure 2a, Ramirez (2019) and Hwang et al. (2021), which are not repeated here for brevity.

Figure 1b compares the experimental and numerical results from the centrifuge test outlined in the previous section. In general, numerical simulations effectively captured the peak ground acceleration (PGA) at the foundation and roof levels, peak excess pore water pressures (EPWP) in the middle of the liquefiable layer (z = 5 m), permanent foundation settlement, and tilt observed experimentally. However, the transient tilt was slightly underestimated compared to the

centrifuge recordings. The presence of a thick liquefiable layer caused a significant degree of soil softening and de-amplification of accelerations propagating from the base to the foundation, which the numerical model did not adequately capture. Consequently, this discrepancy further increased the accelerations at the foundation and roof level near  $T_p$  compared to the experimental results. Overall, however, the validation exercise (with and without DGCs) demonstrated the capability of the numerical setup and calibrated soil constitutive model to capture the observed experimental trends in terms of accelerations, pore pressures, and permanent foundation settlement and tilt.

After validation, a numerical parametric study was conducted to evaluate the efficiency of DGCs in mitigating the liquefaction hazard within realistic interlayered liquefiable deposits and the resulting deformations below the foundation and transferred to overlying structures. A schematic illustration of a typical 3D model used in this study is shown in Figure 2a.

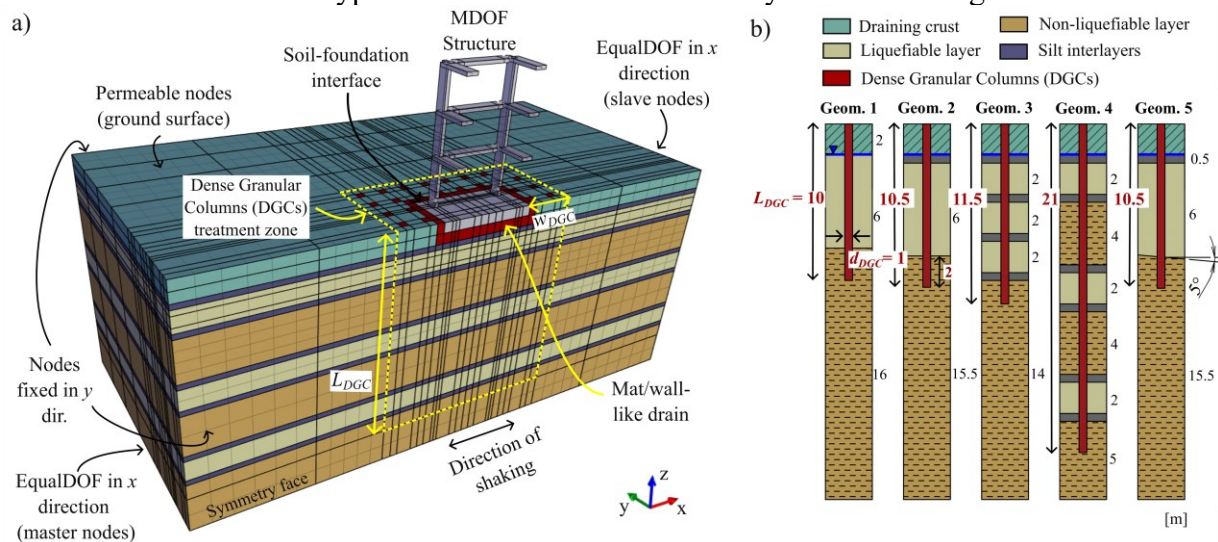


Figure 2. a) Schematic view of a typical 3D numerical model simulating the response of a soil-foundation-structure system mitigated with DGCs, b) geometric configurations of the soil profiles and DGCs characteristics considered in the numerical parametric study (all dimensions are in meters).

Figure 2b illustrates the simplified representations of the layering of five soil profile geometries considered in this study that were designed to account for 2D stratigraphic variabilities commonly found in realistic deposits (e.g., in terms of hydraulic conductivity, layer thickness, relative density, number of critical layers). These soil profiles ranged from single uniform layers (Geometries 1 & 2) to highly stratified deposits (Geom. 3 & 4) or non-uniform liquefiable layers (Geom. 5) with a lower boundary layer sloped at 5°. These comprised loose layers of Ottawa sand with  $D_r = 40\%$ , representing the critical liquefiable layers, and denser layers with  $D_r = 90\%$ . Coarse and dense Monterey sand ( $D_r = 90\%$ ) was employed as a draining crust. Thin (0.5 m-thick) silica silt layers with low permeability were introduced between or within the liquefiable layers to modify the system's drainage capacity or critical layer continuity. The DGC material was a uniform, clean, fine gravel column. The calibrated model parameters used for all soil layers were adopted from Badanagki et al. (2018), Hwang et al. (2021), and Tiznado et al. (2021). The total height of all soil profiles was kept constant at 24 m, and the water table depth ( $z_{gwt}$ ) was 2 m. The dimensions of the soil domain were determined as 6B and 3B (where B is the foundation width) in length and width, respectively, based on Hwang et al. (2022).

This preliminary sensitivity study aimed to account for variations in the geometry and characteristics of the DGC that have previously been shown as influential (e.g., Tiznado et al. 2021). These variables included the area replacement ratio  $(A_r)$ , the ratio of hydraulic conductivity of the DGC to that of the surrounding critical soil layer  $(k_r)$ , the ratio of the maximum shear modulus of the DGC to that of the surrounding critical soil layer  $(G_r)$ , and densification of critical layers induced by DGC installation  $(D_{r,DS})$ .  $A_r$  ranged from 10 to 20%, consistent with field case histories involving DGCs in the literature (Tiznado et al., 2020). The  $G_r$  values ranged from 2 to 8, based on Baez (1995) and Tiznado et al. (2020). The selected values of  $k_r$  represented three scenarios of DGC drainage capacity: complete clogging with fines  $(k_r = 0)$ ; clogging with the surrounding soil, resulting in no change in drainage capacity  $(k_r = 1)$ ; and no clogging, representing enhanced drainage  $(k_r = 100)$ . Finally,  $D_{r,DS}$  was estimated at 90% based on an initial  $D_{r,c}$  of 40% and  $A_r$  values of 10-20%, following Baez (1995).

For all soil profiles, the depth of treatment ( $L_{DGC}$ ) was designed to fully cover the thickness of the critical layers, following the recommendations from JGS (2018), with an additional 2 m extension into the denser layer below. The range of  $L_{DGC}$  varied from 10 to 21 m to cover the deepest critical layer(s), and the columns extended to the ground surface. Laterally, the treatment zone extended beyond the foundation edge by B/2 in both horizontal directions ( $w_{DGC}$ ). When applicable, the zone of densification resulting from column installation was confined to the loose layers in the improved area. To simplify the mesh, a square-shaped drain cross-section with a 1 m width ( $d_{DGC}$ ) was used, while the columns were positioned with a center-to-center spacing of 1.6 m. In addition, a 1 m-thick mat and wall-like drains were installed around the foundation in all models, as shown in Figure 2a. The DGC and the surrounding soil elements were assumed to be tied together at their nodes (i.e., no interface elements).

The parametric study used the maximum rotated horizontal component (RotD100) PGA of the 2011 Christchurch earthquake recorded at the PARS station, which has a moment magnitude  $(M_w)$  of 6.0 and a distance to rupture (R) of 3.6 km. To obtain the within-rock motion as input to the numerical model's rigid base, deconvolution was performed for each soil profile using 1D equivalent-linear site response analyses in DEEPSOIL 7.0 (Hashash et al. 2020).

# INSIGHTS FROM THE NUMERICAL PARAMETRIC STUDY ON DGC PERFORMANCE

To evaluate the effect of DGCs on the primary demand parameters of interest, Figure 3 presents the numerical results obtained for a baseline soil profile featuring a single uniform liquefiable layer (Geom. 1) with  $z_{gwt} = 2$  m. The results include predictions of settlement ( $\delta$ ), tilt ( $\theta$ ), excess pore water pressure ratio ( $r_u$ ) time histories, and spectral accelerations ( $S_a$ ) on the roof and foundation of the structure. We compare a "baseline" mitigation scenario characterized by  $A_r = 10\%$ ,  $k_r = 100$ ,  $k_r = 2$ , and  $k_r = 20\%$ , with an unmitigated case ("no mitigation" or NM). Additionally, we explore the effects of variations in DGC properties, such as  $k_r = 20\%$ ,  $k_r = 0$  or 1, and  $k_r = 20\%$ , as well as the influence of raising the water table ( $k_r = 0$ ) m from 2 m).

Figure 3 shows that the mitigation scenarios with enhanced drainage ( $k_r = 100$ ) effectively limited the amplitude and duration of  $r_u$  accumulation in the critical layer(s), thereby reducing foundation  $\delta$  compared to an unmitigated structure. The most significant reduction in foundation settlement (i.e.,  $\delta_{DGC}/\delta_{NM}$  &  $\delta_{NM} = 17$  cm) for  $z_{gwt} = 2$  m was observed when increasing  $A_r$  from 10 to 20% or considering installation-induced ground densification ( $D_{r,DS} = 90\%$ ). However, in cases with clogging (i.e.,  $k_r = 0$  or 1), shear reinforcement provided by the DGCs alone did not produce

any visible improvements on  $\delta$  compared to the unmitigated soil profile (even for  $G_r$  as high as 8).

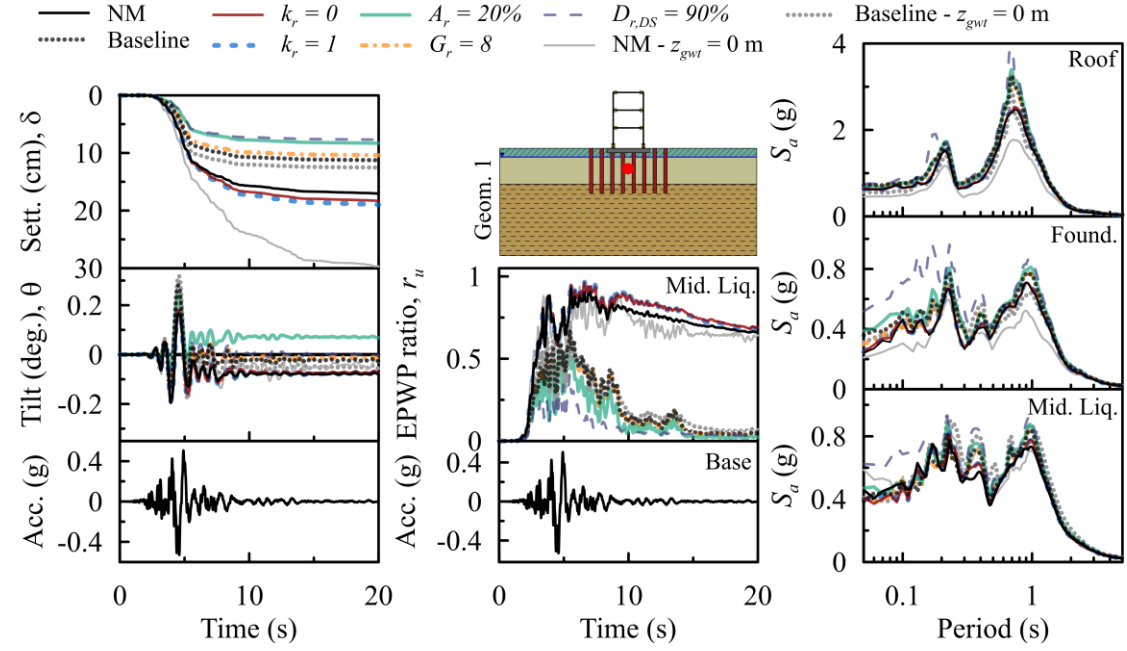


Figure 3. Foundation settlement  $(\delta)$ , tilt  $(\theta)$ , and excess pore water pressure ratio  $(r_u)$  time histories (EPWP), and 5%-damped acceleration response spectra  $(S_u)$  at different locations, as a function of dense granular column properties, compared with an unmitigated model (NM), a baseline mitigation scenario (Baseline; where  $A_r = 10\%$ ,  $k_r = 100$ ,  $G_r = 2$ , and  $D_{r,c} = 40\%$ ), and a case with a lower water table depth at  $z_{gwt} = 0$  m, for soil profile geometry 1.

In general, the scenarios with enhanced drainage ( $k_r = 100$ ) exhibited a slight amplification of the foundation's transient tilt, while the permanent tilt remained unchanged. The baseline mitigation scenario,  $G_r = 8$ , and  $D_{r,DS} = 90\%$ , provided minor reductions in permanent tilt compared to the unmitigated case. Importantly, DGCs without clogging amplified the accelerations from the foundation to the roof near the motion's predominant period ( $T_p = 0.9$  s) and at a period slightly greater than the fundamental period of the structure ( $T_0 = 0.56$  s) due to reduced damping within the treated soil. In addition,  $D_{r,DS} = 90\%$  significantly increased the foundation  $S_a$  at shorter periods compared to other DGC mitigation mechanisms due to the densified soil's greater initial shear stiffness and strength.

Finally, raising the water table depth from 2 to 0 m increased the settlement of the unmitigated case  $\delta_{NM}$  by approximately 75% ( $\delta_{NM} = 30$  cm). This reduction was attributed to reduced effective normal stresses below the foundation, which increased the extent of softening and damping within the soil at shallower depths, also slightly de-amplifying the accelerations transmitted to the superstructure. For this water table depth, implementing DGCs reduced the foundation settlement by up to a  $\delta_{DGC}/\delta_{NM}$  factor of 0.42.

Figure 4a compares normalized engineering demand parameters ( $EDP_{DGC}/EDP_{NM}$ ) to provide a more comprehensive assessment of the seismic performance of DGCs in realistic liquefiable soil profiles for the structure and ground motion considered. The figure includes the median predictions from the five soil profile geometries with  $z_{gwt} = 2$  m shown in Figure 2b, presented as a function of the different mitigation scenarios. We use the median value to provide a representative value of the central tendency of the data that is less sensitive to extreme values. The EDPs analyzed in this study are the normalized permanent foundation settlement ( $\delta$ ),

permanent tilt ( $\theta$ ), peak pore pressure ratio in the middle of the liquefiable layer (or at a depth of 11.5 m for Geom. 4) ( $r_{u \, Mid. \, Liq}$ ), and roof 5%-damped  $S_a$  at the structure's natural period ( $S_{a \, Roof-T0}$ ).

To estimate the potential reduction in ejecta severity under the foundation, we use the ejecta potential index (EPI) and severity classes proposed by Hutabarat et al. (2021), which have been shown to correlate well with previous case histories of surface ejecta. The EPI is calibrated for simulations of 150 s, as field observations of earthquakes indicate that cracks start forming in the crust 2-3 minutes after shaking. To reduce the computational cost associated with 3D modeling and estimate  $EPI_{UB}$ , a unit cell model with a surcharge to represent the foundation's contact pressure was adopted to model the soil mitigation system. This approximation of ejecta potential is necessary, as a continuum FEA cannot directly predict ejecta formation within the mesh.

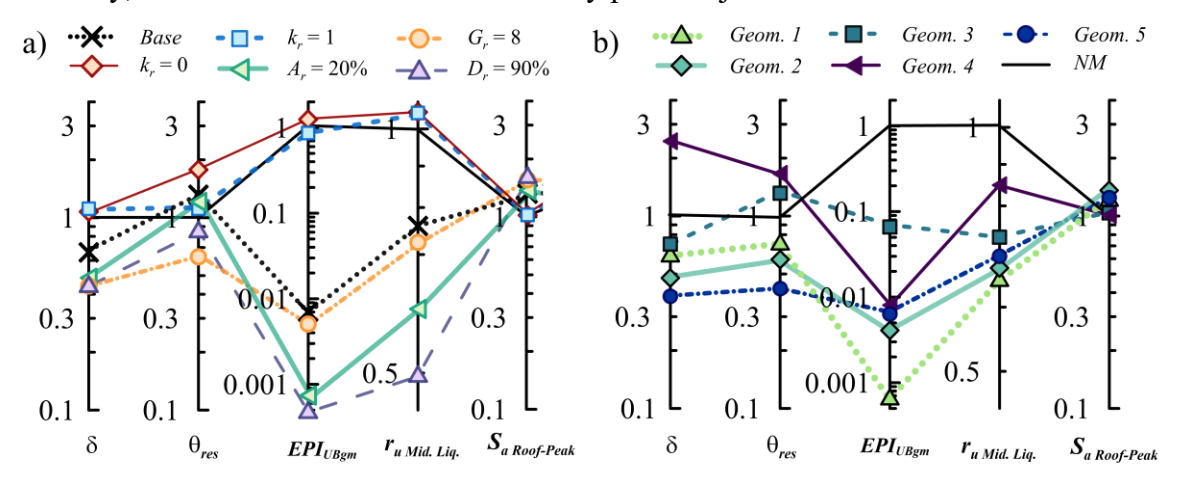


Figure 4. Comparison of median normalized permanent foundation settlement  $(\delta)$ , permanent tilt  $(\theta)$ , ejecta potential index under the center of the foundation  $(EPI_{UB})$ , peak pore pressure ratio in the middle of the liquefiable layer  $(r_{u\ Mid.\ Liq})$ , and roof 5%-damped response spectra at the structure's natural period  $(S_{a\ Roof-T\theta})$  [in terms of the ratio of mitigated versus unmitigated], as a function of: a) dense granular column properties for all soil profile geometries; and b) soil profile geometry for all mitigation configurations.

Figure 4a illustrates the efficiency of drainage-based mitigation scenarios ( $k_r = 100$ ) in decreasing  $\delta$  compared to untreated deposits across varying soil profile geometries. For instance, the median value of  $\delta_{DGC}/\delta_{NM}$  was reduced from 0.7 (baseline scenario;  $A_r = 10\%$ ,  $k_r = 100$ ,  $G_r =$ 2, and  $D_{r,c} = 40\%$ ) to about 0.4 for mitigation scenarios with  $A_r = 20\%$ ,  $k_r = 100$ ,  $G_r = 8$ , or when combined with densification ( $D_{r,DS} = 90\%$ ). Soil drains with  $k_r = 100$  could also significantly reduce  $r_u$  within liquefiable layers, with  $r_{uDGC}/r_{uNM}$  ranging from 0.75 (Baseline) to 0.5 ( $D_{r.DS}$ = 90%), reducing the likelihood of triggering and significant strength loss (consistent with numerical results of single column analyses by Tiznado et al. 2021). On the other hand, clogged drains did not visibly improve the examined EDPs, emphasizing the importance of installing adequate filters around the drains to prevent clogging to the extent possible. In fact, clogging by fines could adversely affect overlying structures, amplifying the permanent foundation tilt by up to 1.8 times  $(k_r = 0)$  that of the untreated structure due to a slight increase in  $r_u$ . On the other hand, both the baseline and  $A_r = 20\%$  mitigation scenarios with or without drainage were found to amplify the permanent tilt of the foundation by up to  $\theta_{DGC}/\theta_{NM} = 1.3$ . This amplification was due to an increased acceleration demand on the superstructure caused by reduced damping in the underlying treated soil, increasing the P- $\Delta$  effects that lead to rotation. However, the larger shear reinforcement and stiffness provided by the  $G_r = 8$  or  $D_{r,DS} = 90\%$  mitigation scenario reduced the permanent tilt by up to 0.6 compared to its untreated counterpart for the ground motion considered. In general, all cases, particularly treatment with  $k_r = 100$ , showed notable amplification of the accelerations transmitted to the superstructure, which needs to be considered in the structural design of mitigated foundations.

Moreover, the findings highlight the effectiveness of the mitigation scenarios with enhanced drainage in reducing the severity of ejecta potential, particularly under the foundation, as evidenced by the reduced normalized  $EPI_{UB}$  values. Based on the ejecta severity thresholds proposed by Hutabarat et al. (2021),  $D_{r,DS} = 90\%$  was found to be the most effective by reducing the ejecta severity class from "extreme" (unmitigated) to "none". A reduction to the "minor" severity class was observed with an increase of  $A_r$  to 20%, while both the baseline and  $G_r = 8$  scenarios were associated with "moderate" ejecta.

Figure 4b compares the EDPs across different soil profile geometries, displaying the median response of all mitigation configurations, to evaluate the effect of stratigraphic variability on DGC performance. Overall, the unmitigated permanent foundation settlements ranged from 2 cm to 31 cm (i.e.,  $\delta_{NM} = 17$  cm, 31 cm, 18 cm, 2 cm, and 30 cm for soil Geom. 1 through 5, respectively), highlighting the significant variability in foundation behavior with stratigraphic variabilities. Introducing thin silt interlayers above the thicker, continuous critical liquefiable layers in both Geom. 2 and 5 led to an increased accumulation of excess pore pressures beneath the foundation and slower dissipation rates compared to Geom. 1. As a result, the largest  $\delta_{NM}$  values were obtained for these soil profiles. However, DGC mitigation of these deposits showed notable improvements with respect to  $\delta_{DGC}/\delta_{NM} = 0.3$ , as the extension of the drains through the silt cap facilitated faster dissipation of excess pore pressures within the uniform layer beneath the foundation.

Geom. 4, characterized by 3x2-m thick liquefiable layers spatially distributed throughout the soil profile's entire depth, displayed base isolation effects due to the faster liquefaction of the deeper critical layer. This isolation effect reduced the amplitude of accelerations propagating to the surface, minimizing softening below the foundation at shallow layers compared to the other soil profiles. As a result, the predicted permanent foundation settlement was significantly lower in these geometries. However, the treatment of Geom. 4 encouraged a redistribution of excess pore water pressures from the shallow critical layers to thicker, denser layers. Although minor, this increased softening in a larger volume of soil contributed to increasing the foundation's permanent settlement with a median value of  $\delta_{DGC}/\delta_{NM} = 1.6$ .

A slight amplification of the permanent  $\theta$  could be observed with mitigation for Geom. 1 to 4. However, the initial  $\theta_{NM}$  values were shown to be generally negligible (i.e.,  $\theta_{NM} = 0.08^{\circ}$ ,  $0.04^{\circ}$ ,  $0.03^{\circ}$ , and  $0.01^{\circ}$  for soil Geom. 1 through 5, respectively). This tilt range is expected for isolated and symmetric structures on perfectly uniform liquefiable layers (see Bullock et al. 2019). Hence, the amplification due to DGCs may simply be within the range of numerical error expected for such small demand parameters. In cases where  $\theta_{NM}$  was expected to be critical and concerning, such as with non-uniform liquefiable layers (Geom. 5;  $\theta_{NM} = 0.8^{\circ}$ ), DGCs were generally successful in reducing the foundation's permanent tilt up to  $\theta_{DGC}/\theta_{NM} = 0.3$  for the conditions considered.

Overall, DGCs decreased the severity of ejecta (or EPI) and  $r_u$  accumulation in all soil profiles, as previously noted. However, the results suggest that significant soil softening remained in the looser layers of the soil profiles with multiple silt interlayers, which limited pore pressure dissipation. The predicted peak median  $r_u$  values at the end of shaking with mitigation for Geom.

3 and 4 were 0.8 and 0.9, respectively. The prolonged duration of high pore pressures and increased damping in the mitigated Geom. 3 and 4 soil layers limited the amplification of accelerations transmitted to the overlying structure compared to the other soil profiles considered.

### **CONCLUSIONS**

In this paper, a limited set of 3D, fully-coupled, effective-stress, finite element simulations, validated with centrifuge experiments, is used to evaluate the impact of DGC mitigation properties and stratigraphic variability on the effectiveness of various mitigation mechanisms provided by DGCs in improving building performance. The results reveal that DGCs with enhanced drainage (no clogging) effectively reduce the foundation's permanent settlement, excess pore pressure ratios, and ejecta severity compared to an unmitigated structure, particularly for DGCs with  $A_r$  of 20% or combined with densification. However, the performance of DGCs was shown to vary significantly depending on the soil profile and mitigation properties considered, potentially leading to adverse effects on overlying structures, such as amplifications of roof accelerations. The findings of this limited sensitivity study emphasize the complexities in mitigating liquefaction-induced damage and highlight the need for a comprehensive understanding of the behavior of interlayered, realistic deposits to improve the performance of the soil-foundation-mitigation systems. Further research incorporating a broader range of soil profiles, soil types, mitigation properties or geometries, building properties, and ground motion characteristics is required for improved guidelines on performance-based mitigation procedures.

# **ACKNOWLEDGEMENTS**

Funding from the Natural Sciences and Engineering Research Council of Canada (NSERC) is gratefully acknowledged. This work utilized the Alpine high performance computing resource at the University of Colorado Boulder. Alpine is jointly funded by the University of Colorado Boulder, the University of Colorado Anschutz, Colorado State University, and the National Science Foundation (award 2201538).

### REFERENCES

- Badanagki, M., Dashti, S., and Kirkwood, P. (2018). "Influence of dense granular columns on the performance of level and gently sloping liquefiable sites." *J. Geotech. Geoenviron. Eng.*, 144(9), 04018065.
- Badanagki, M., Dashti, S., Paramasivam, B., and Tiznado, J. C. (2019). "How do granular columns affect the seismic performance of non-uniform liquefiable sites and their overlying structures?" *Soil Dyn. and Earth. Eng.*, 125, 105715.
- Baez, J. I. 1995. "A design model for the reduction of soil liquefaction by vibro-stone columns." Ph.D. thesis, Dept. of Civil and Environmental Engineering, Univ. of Southern California.
- Beyzaei, C. Z., Bray, J. D., Cubrinovski, M., Riemer, M., and Stringer, M. (2018). "Laboratory-based characterization of shallow silty soils in southwest Christchurch." *Soil Dyn. and Earth. Eng.*, 110, 93-109.
- Bullock, Z., Dashti, S., Karimi, Z., Liel, A., Porter, K., and Franke, K. "Probabilistic Models for Residual and Peak Transient Tilt of Mat-Founded Structures on Liquefiable Soils." *J. Geotech. Geoenviron. Eng.*, 145(2).
- Cubrinovski, M., A. Rhodes, N. Ntritsos, and S. Van Ballegooy. (2017). "System response of

- liquefiable deposits." *Proc., 3rd Int. Conf. on Perf.-Based Design in Earthq. Geotech. Eng.* London: International Society for Soil Mechanics and Geotechnical Engineering.
- Elgamal, A., Yang, Z., and Parra, E. (2002). "Computational modeling of cyclic mobility and post-liquefaction site response". *Soil Dyn. Earthq. Eng.*, 22(4), 259-271.
- Hashash, Y.M.A., Musgrove, M.I., Harmon, J.A., Ilhan, O., Xing, G., Numanoglu, O., Groholski, D.R., Phillips, C.A., and Park, D. (2020). "DEEPSOIL 7, User Manual". Urbana, IL, Board of Trustees of University of Illinois at Urbana-Champaign.
- Hutabarat, D., and Bray, J. D. (2021). "Effective stress analysis of liquefiable sites to estimate the severity of sediment ejecta." *J. Geotech. Geoenviron. Eng.*, 147(5), 04021024.
- Hwang, Y. W., Bullock, Z., Dashti, S., and Liel, A. (2022). "A Probabilistic Predictive Model for Foundation Settlement on Liquefiable Soils Improved with Ground Densification." *J. Geotech. Geoenviron. Eng.* 148(5), 04022017.
- Hwang, Y. W., Ramirez, J., Dashti, S., Kirkwood, P., Liel, A., Camata, G., and Petracca, M. (2021). "Seismic interaction of adjacent structures on liquefiable soils: insight from centrifuge and numerical modeling." *J. Geotech. Geoenviron. Eng.*, 147(8), 04021063.
- Ishihara, K. (1985). "Stability of natural deposits during earthquakes." *Proc., 11th Int. Conf. on Soil Mech. and Geotech. Eng.*, 1, 321-376
- JGS, Japanese Geotechnical Society. *Remedial measures against soil liquefaction*. Rotterdam: A.A. Balkema; 1998.
- Kokusho, T., and Fujita, K. (2011). "Water films involved in post-liquefaction flow failure in Niigata City during the 1964 Niigata Earthquake". *Proc.*, 4th Int Conf on Recent Advances in Geotech Earthq Eng and Soil Dyn, 25.
- Luque, R., and Bray, J. D. (2017). "Dynamic analyses of two buildings founded on liquefiable soils during the Canterbury earthquake sequence." *J. Geotech. Geoenviron. Eng.*, 143(9).
- Mazzoni, S., McKenna, F., Scott, M. H., and Fenves, G. L. (2006). *Open system for earthquake engineering simulation user command-language manual*. Pacific Earthquake Engineering Research Center, University of California, Berkeley, OpenSees version, 1(3).
- Nikolaou, S., X. Vera-Grunauer, and R. Gilsanz. (2016). GEER-ATC earthquake reconnaissance, April 16, 2016, Muisne, Ecuador. Rep. No. GEER-049. Geotechnical Extreme Events Reconnaissance Association.
- O'Rourke, T. D, and Lane, P. A. (1989). Liquefaction hazards and their effects on buried pipelines. National Science Foundation, Washington, DC., 204.
- Olarte, J., Paramasivam, B., Dashti, S., Liel, A., and Zannin, J. (2017). "Centrifuge modeling of mitigation-soil-foundation-structure interaction on liquefiable ground." *Soil Dyn. Earthq. Eng.*, 97, 304-323.
- Ramirez, J. (2019). "Numerical modeling of the influence of different liquefaction remediation strategies on the performance of potentially inelastic structures." Ph.D. Dissertation, Dept. of Civil, Env., and Arch. Eng., Univ. of Colorado Boulder.
- Tiznado, J. C., S. Dashti, C. Ledezma, B. P. Wham, and M. Badanagki. (2020). "Performance of embankments on liquefiable soils improved with dense granular columns: Observations from case histories and centrifuge experiments." *J. Geotech. Geoenviron. Eng.*, 146 (9): 04020073.
- Tiznado, J. C., S. Dashti, and C. Ledezma. (2021) "Probabilistic Predictive Model for Liquefaction Triggering in Layered Sites Improved with Dense Granular Columns." *J. Geotech. Geoenviron. Eng.*, 147(10), 04021100.
- Yang, Z., Lu, J., & Elgamal, A. (2008). OpenSees soil models and solid-fluid fully coupled elements. User's Manual. Ver, 1, 27.